Published in final edited form as:
Kidney Int. 2013 March ; 83(3): 426–437. doi:10.1038/ki.2012.379.

The cytoplasmic protein Pacsin 2 in kidney development and injury repair

Gang Yao[1], **Annouck Luyten**[1], **Ayumi Takakura**[1], **Markus Plomann**[2], and **Jing Zhou**[1]

[1]Renal Division, Department of Medicine, Brigham and Women's Hospital, Harvard Medical School, Boston, Massachusetts, USA and [2]Institute for Biochemistry and Center for Molecular Medicine Cologne (CMMC), University of Cologne, Cologne, Germany

Abstract

The protein kinase C and casein kinase 2 substrate in neurons (Pacsin) is a subfamily of membrane-binding proteins that participates in vesicle trafficking and cytoskeleton organization. Here, we studied Pacsin 2 in kidney development and repair following injury. In the postnatal developing kidneys, Pacsin 2 was found to be expressed in both ureteric bud- and mesenchyme-derived structures including proximal and distal tubules, Bowman's capsule, and the glomerular tuft. In the adult kidney, its expression was decreased in proximal tubules but increased in glomerular tuft when compared to that in the developing kidneys. Interestingly, Pacsin 2 expression was significantly upregulated during the repair phase after ischemia–reperfusion injury, especially on the apical brush border of proximal tubules that experienced massive damage. Pacsin 2 localized to the primary cilia of renal epithelial cells. Knockdown of Pacsin 2 by shRNA did not affect the cell cycle or cell polarity; however, it increased the length of primary cilia, and resulted in significant tubulogenic defects in three-dimensional cell culture. Thus, we propose that Pacsin 2 contributes to kidney development and repair in a nephron-specific manner.

Keywords

renal development; renal injury; renal ischemia–reperfusion; renal tubular epithelial cells

Pacsin 2 is a member of the Pacsin (protein kinase C and casein kinase 2 substrate in neurons) protein family. To date, there are three known members in the Pacsin protein family. Pacsin 1 localizes specifically to neurons, Pacsin 3 is mainly detected in the lung and the muscle, and Pacsin 2 has a ubiquitous distribution and has a high expression in the kidney.[1] Pacsin family proteins are characterized by a highly conserved amino terminal Bin-Amphiphysin-Rvs (F-Bar) domain. Structural studies revealed that the F-Bar domain is required for dimerization to form a crescent or S-shaped structure and is essential for sensing, stabilizing, and inducing changes in membrane topology such as during

Correspondence: Jing Zhou, Harvard Institutes of Medicine, Room 522, 4 Blackfan Circle, Boston, Massachusetts 02115, USA. Zhou@rics.bwh.harvard.edu.

DISCLOSURE All the authors declared no competing interests.

endocytosis.[2–5] Pacsins localize to sites of high actin turnover, such as filopodia tips and lamellipodia,[6] and directly interact via their Src-homology 3 domain with the neural Wiskott–Aldrich syndrome protein (N-WASP),[1] which is a potent activator of the Arp2/3 (actin-related protein 2/3) complex that functions in actin filament nucleation,[6–8] the rate-limiting step for actin filament polymerization.[9] The Pacsin 1–N-WASP–Arp2/3 complex–dependent actin nucleation is essential for proper neuromorphogenesis; similar to the loss of N-WASP and Arp3, the loss of Pacsin 1 results in improper axon development.[10] Interestingly, N-WASP deficiency causes tubulogenesis defects in Madin–Darby canine kidney cells and reduces the branching and tubule extension in three-dimensional (3D) cultures.[11] Previous studies on Pacsin 2 mostly used nonepithelial cell models.[1,12–16] Its expression in kidney development and repair after injury is not known. Whether Pacsin 2 plays a role in tubulogenesis has not been investigated previously.

Here, we reported that Pacsin 2 is differentially expressed in different nephron segments. Its expression in specified nephron segments coincides with kidney development and kidney repair after ischemia–reperfusion injury (IRI). Pacsin 2–deficient murine inner medullary collecting duct 3 (mIMCD3) cells exhibit disordered tubule formation, resulting in multilumen structures in 3D collagen gels. In this study, we also show that Pacsin 2 localizes on the primary cilia and modulates cilium length in kidney epithelial cells. The primary cilium defects cause a number of human genetic diseases, including polycystic kidney diseases and Bardet–Biedl syndrome, collectively termed ciliopathy.[17] Taken together, our results suggest that Pacsin 2 contributes to kidney development and repair.

RESULTS

Pacsin 2 expression and localization in kidney epithelial cells

Virtually nothing is known about Pacsin 2 in the kidney. As a first step to study its role in the kidney, we double-stained kidney sections from newborn and 1- to 3-week-old mice with Pacsin 2 antibodies and nephron segment markers. In kidneys from newborn to 1-week-old mice, Pacsin 2 expression was seen at the apical membrane in both Lotus tetragonolobus agglutinin–positive (LTA^+) proximal and Dolichos biflorus agglutinin–positive (DBA^+) collecting tubules. The apical expression of Pacsin 2 in LTA- and DBA-positive tubules was also seen in embryonic day 15.5 and 18.5 kidneys (Supplementary Figure S1 online). At 3 weeks of age, however, Pacsin 2 expression is significantly decreased in LTA^+ proximal tubules, and its localization becomes mostly cytoplasmic, with only weak signals on the apical membrane in a small fraction of (~5%) LTA^+ proximal tubules. In contrast, the apical membrane expression of Pacsin 2 in DBA^+ collecting tubules is retained and became even stronger (Figure 1a and b; and data not shown). Consistently, western blot analysis confirmed a remarkable reduction of Pacsin 2 in 3-week-old kidneys compared with the newborn kidneys (Supplementary Figure S2 online).

Nephrogenesis continues in the first 2 weeks of postnatal life in rodents. To investigate a potential role of Pacsin 2 in this process, we examined the extreme cortex of newborn mouse kidneys where the nephrogenic zone lies. We observed strong apical labeling of Pacsin 2 in ureteric bud and its derivative structures. Only weak signals were seen in newly formed nephron structures such as the S-shaped bodies, which are negative for Pacsin 2 (Figure 2a).

In the cortical medullar region of postnatal kidneys, Pacsin 2 expression is detectable in the parietal epithelial cells of the Bowman's capsule but not in the glomerulus. It is noteworthy that Pacsin 2 expression becomes detectable in both the podocytes of the glomerular tufts and parietal cells in adult kidneys, although its expression in proximal tubules becomes undetectable (Figure 2b, and Supplementary Figure S3 online).

Primary cilia act as mechanosensors and/or chemosensors and transduce signals from the extracellular environment into the cell to regulate a number of important signaling events. As Pacsins may localize to the centrosomes, which is a barrel-shaped microtubule-based structure critical for cell division and ciliogenesis,[18] we tested whether Pacsin 2 is on the primary cilia of kidney epithelial cells. By double-labeling cells with Pacsin 2 and acetylated α-tubulin, a marker for the axoneme of the primary cilium, we found that Pacsin 2 colocalized with acetylated α-tubulin on the shaft of the primary cilia in mIMCD3 cells (Figure 3a). Its expression on primary cilia is weakly detectable in tubular epithelial cells *in vivo* (Figure 3b). Pacsin 2 ciliary localization was further confirmed by double labeling of Pacsin 2 with γ-tubulin, a marker for the basal body (Figure 3a).

Pacsin 2 knockdown does not affect cell proliferation and cell cycle in mIMCD3 cells

To assess the function of Pacsin 2 in kidney tubular cells, we silenced Pacsin 2 expression in mIMCD3 cells by small hairpin RNA interference (shRNA) and established four stable knockdown clones and six scrambled controls. Western blot analysis verified a significant decrease in Pacsin 2 protein abundance in these knockdown cell lines (Figure 4a). Semiquantitative reverse transcriptase-PCR confirmed that Pacsin 2 mRNA was also reduced (Figure 4b) in these four knockdown cell lines. Immunofluorescent analysis with a Pacsin 2–specific antibody revealed a significant reduction of the Pacsin 2 signal in Pacsin 2 knockdown cells compared with control mIMCD3 cells (Figure 4c). MTT (3-[4,5-dimethylthiazol-2-yl]-2,5-diphenyl-tetrazolium bromide) cell proliferation assay and fluorescence-activated cell sorting (FACS) analysis revealed that neither the cell proliferation rate (Figure 4d) nor the cell cycle profile (Figure 4e) of Pacsin 2 knockdown cells was significantly altered as compared with control cells.

Pacsin 2 knockdown mIMCD3 cells process longer primary cilia

Surprisingly, with acetylated α-tubulin as a marker, we found that the primary cilia in Pacsin 2 knockdown cells were ~31% longer than those in control cells. This difference is statistically significant ($P<0.01$), as determined by Student's *t*-test (Figure 4f and g).

Pacsin 2 knockdown disrupts tubulogenesis in 3D culture

mIMCD3 epithelial cells have been used as an *in vitro* model of the kidney tubulogenesis system. When cultured in a collagen gel matrix, mIMCD3 cells form fluid-filled branching tubule-like structures that comprise a single layer of polarized cells, resembling renal tubules. We assessed the tubulogenic potential of Pacsin 2 using this assay. After culturing in 3D type I collagen gels for 12 days, the control mIMCD3 cells formed branching tubules lined by a single layer of epithelial cells with primary cilia protruding toward the lumen (88% of the structures; Figure 5a1, b, and c1 and 2). This process, however, was defective in all three stable Pacsin 2 knockdown cell lines tested. Most of the structures formed by

Pacsin 2 knockdown cells were cell clusters often containing multilumens (65%) or cell chains (17%) (Figure 5a2–5, b, and c3–8). The small fraction of the Pacsin 2 knockdown cells that were able to form tubule-like structures/cords showed reduced branching with no lumen formation (18%). These cords usually exhibited blunt ends, indicating that there was a branching defect (Figure 5a5 and c3).

Pacsin 2 knockdown affects cell invasion but not cell polarity

Tubulogenesis requires coordinated invasion of cells through the extracellular matrix. Pacsin family proteins interact with N-WASP and modulate actin nucleation. Given the fact that N-WASP deficiency in Madin–Darby canine kidney cells led to a defect in directed cell invasion, we examined whether Pacsin 2 is required for this process. Therefore, we performed an invasion assay in which subconfluent cells travel through an 8-μm porous filter that was coated with type I collagen. In this assay, an identical number of both control and Pacsin 2 knockdown cells were plated on the apical surface of the filter. The hepatic growth factor (HGF) is only added into the medium of the lower chamber to attract cells to travel through the filter. Cells that traversed the filter were visualized on the opposite surface of the filter by Giemsa stain. After 16 h of culture, there was a remarkable reduction of Pacsin 2 knockdown cells that had traveled toward the opposite side of the filter (Figure 6a and b).

Epithelial tubulogenesis requires strict control of cell–cell adhesion and cell polarity.[11,19] To examine the formation of the adherent/tight junctions and cell polarity, we used ZO1 and E-cadherin as respective markers to stain cells grown on permeable filters, which allows for better maintenance of cell polarity. We did not detect obvious differences in the expression of these junctional markers between Pacsin 2 knockdown cells and control mIMCD3 cells (Figure 6c, and Supplementary Figure S4a online). To determine whether there was a change in cell polarity and cell–cell junction, we stained cells cultured in 3D collagen gels with ZO1 and β-catenin. Consistent with data from 2D cultures, both ZO1 and β-catenin preserved a normal localization in Pacsin 2 knockdown mIMCD3 cells compared with control mIMCD3 cells in the tubulogenesis assay (Figure 6d, and Supplementary Figure S4b online). These data suggest the preservation of apical–basal cell polarity in Pacsin 2 knockdown cells, which is consistent with the presence of primary cilia on the apical side of the multilumen structures in this assay (Figure 5b7).

Pacsin 2 expression is upregulated after renal IRI

IRI is the most common cause of acute renal failure. It is characterized by rapid loss of renal function and tubular damages. Upon removal of the deleterious cause, the injured kidneys start a rapid repair process—the resident surviving tubular cells proliferate and migrate to replace the lost or damaged cells—24–48 h after injury at the proximal tubules of the outer medulla where the injury is maximum.[20,21] To further investigate the role of Pacsin 2 during kidney injury and the repair process, we performed unilateral renal IRI on 3-month-old wild-type mice.[21] At 48 h after IRI, mice were killed and kidneys were harvested for immunostaining. In contralateral nonischemic kidneys that served as controls, Pacsin 2 was detected in LTA^+ proximal tubules at basal levels in the cytoplasm. In contrast, strong Pacsin 2 labeling highlights the brush border of most LTA^+ tubules in injured kidneys

(Figure 7a, insert, and Supplementary Figure S5a online). A more intense apical Pacsin 2 signal was also observed in DBA^+ tubules in ischemic kidneys compared with that in the nonischemic control kidneys (Figure 7b and Supplementary Figure S5b online). There is little or no Pacsin 2 signal in severely injured tubules with severe cell death or a denuded basement membrane (data not shown). Consistently, western blot analysis revealed a remarkable increase in the protein levels of Pacsin 2 in injured kidneys compared with the nonischemic control kidneys (Figure 7c and d).

DISCUSSION

Here, we report a detailed characterization of Pacsin 2 localization in cultured kidney cells and *in vivo*. We identified Pacsin 2 as a new protein in controlling the formation of kidney tubules and the length of primary cilia in kidney epithelial cells. Moreover, we report a striking upregulation of Pacsin 2 in kidneys after IRI.

During kidney development, mesenchymal cells induce growth and repeated branching of the ureteric bud. Reciprocally, the tips of the branching ureteric bud, where Pacsin 2 is expressed, induce the surrounding mesenchymal cells to condense into renal vesicles, which ultimately differentiate into various segments of the nephron.[22–24] F-actin is known to be expressed apically in the tips of ureteric buds and is essential for branching morphogenesis in the developing kidney.[25] The apical localization of Pacsin 2 in the ureteric buds is consistent with the notion that Pacsin 2 localizes to high actin turnover sites and modulates actin cytoskeleton reorganization. These data suggest that Pacsin 2 may participate in the regulation of branching morpho-genesis in the developing kidney through modulation of the actin cytoskeleton.

Pacsin 2 expression appears to be downregulated in proximal tubules after postnatal kidney development, whereas its apical localization in collecting ducts remains. In embryonic day 15.5 and newborn kidneys, Pacsin 2 is present in the apical membrane in both proximal and collecting tubules in the kidney. In kidneys of ≥3 weeks of age, when postnatal development is complete, Pacsin 2 expression decreases in proximal tubules and becomes more cytoplasmically localized. This is in contrast to a retained apical membrane expression of Pacsin 2 in collecting tubules. These data suggest that Pacsin 2 may have different roles in different nephron segments. Pacsin 2 may be more important in proximal tubules during early postnatal kidney development, and is needed for the maintenance of the structure and function of collecting system in developed kidneys. The presence of Pacsin 2 on both the apical surfaces of parietal epithelial cells of the Bowman's capsule and podocytes of the glomerular tufts of the adult kidney suggests that it might contribute to glomerular filtration in addition to its regulation of tubular structure and/or function.

Depleting Pacsin 2 in mIMCD3 cells leads to remarkable defects in 3D tubulogenesis assays. Pacsin 2–deficient cells form cell cords without an open lumen or cell clusters with irregular multiple lumens, in contrast to the control cells that form tubules with a continuous lumen and elaborate branching. Tubulogenesis requires proper control of cell–cell adhesion, cell polarity, and cell invasion.[11,19] Pacsin 2–depleted cells retain primary cilia on the luminal side and normal localization of markers for cell–cell adhesion and cell polarity when

cultured either on permeable filters or in 3D collagen gels. Therefore, the defect in tubule formation in Pacsin 2–depleted cells likely results from defective cell invasion, similar to the reduced branching and reduced tubule extension observed in 3D culture of N-WASP-deficient Madin–Darby canine kidney cells.[11] Corroboratively, transwell cell invasion assays revealed a remarkable defect in Pacsin 2–depleted mIMCD3 cells (Figure 6a and b). In addition, Pacsin 2 has recently been shown to bind to Rac1 (see ref. 26) and cyclin D1 (see ref. 27) through its Src-homology 3 domain and to negatively regulate cell migration in fibroblast and cancer cells.

Primary cilia may function as mechanosensors and/or chemosensors critical for tubule formation and maintenance in various tissues. We detected Pacsin 2 on the primary cilia and found that Pacsin 2 knockdown cells possess longer (~31%) primary cilia than control cells. Given the requirement of Pacsin 2 for proper activity of the Arp2/3 complex,[1,6–8] it is likely that the defects in the actin cytoskeleton in Pacsin 2 knockdown cells are responsible for the increased length of primary cilia. This is supported by a recent report that shows that Arp3 depletion or inhibition of actin polymerization results in longer cilia by stabilizing a previously unknown pericentrosomal preciliary compartment, a compact vesiculotubular structure that stores ciliary protein during the early phase of ciliogenesis.[28] As the length of primary cilia is tightly controlled and its alteration contributes to the onset and progression of many ciliopathies including polycystic kidney disease, the altered length of primary cilia in Pacsin 2 knockdown cells prompt us to speculate that Pacsin 2–N-WASP–dependent actin nucleation may control the formation and maintenance of the normal kidney tubular structure by modulating the length of the primary cilium, in addition to its key role in cell invasion during tubulogenesis.

IRI is a major cause of acute renal failure in both native kidneys and renal allografts. The kidney exhibits a remarkable capability to recover from acute renal failure after IRI.[20] We found that at 48 h after IRI, Pacsin 2 is strikingly upregulated in proximal tubules of ischemic kidneys, highlighting the brush border that is made up of microvilli. Microvillus is composed of a dense bundle of crosslinked actin filament structure. It increases a cell's surface area, which is especially useful for absorption, secretion, and mechanosensation.[29] Pacsin 2 is known to be enriched at sites with high actin turnover, and to function in the endocytic pathway. Given the weak cytoplasmic expression in proximal tubules in normal adult kidneys, the concentrated Pacsin 2 expression at the brush border in ischemic kidneys suggests that Pacsin 2 may contribute to actin nucleation and/or endocytic processes in proximal tubules during kidney repair.

MATERIALS AND METHODS

Cell culture

The mIMCD3 cells were purchased from ATCC (Manassas, VA) (CRL-2123) and cultured in Dulbecco's modified Eagle's medium/ F12 (50:50) supplemented with 10% fetal bovine serum.

Establishment of stable Pacsin 2 knockdown mIMCD3 cell lines

For the creation of stable cell lines expressing Pacsin 2 shRNA, the pSilencer 2.1-U6-Neo-Pacsin 2 shRNA plasmid was transfected into mIMCD3 cells with Lipofectamine 2000 (Invitrogen, Grand Island, NY) following the manufacturer's instructions. The mouse Pacsin 2 shRNA target sequence is 5'-ATGTCTGTCACCTACGATG-3'. As a control, the pSilencer 2.1-U6-Neo plasmid (Invitrogen) encoding a small hairpin shRNA, which shows no homology to any known gene, was also transfected into cells. Cells were selected using 1 mg/ml G418 in growth medium for 20 days. Surviving clones were transferred onto a 96-well plate, and when confluent they were transferred to 24-, 12-, and 6-well plates. The knockdown efficiency was confirmed by western blotting and semiquantitative PCR analyses.

Western analysis

Briefly, the protein samples were separated on sodium dodecyl sulfate–acrylamide resolving gels and transferred to Hybond ECL (GE Healthcare, Pittsburgh, PA) nitrocellulose membranes. After being blocked with 5% nonfat dry milk in phosphate-buffered saline, the membranes were incubated with the primary antibodies for either 1 h at room temperature or overnight at 4 °C and washed with phosphate-buffered saline/0.1% Tween-20. The membranes were finally incubated with horseradish peroxidase–linked secondary antibodies and visualized with the ECL western blot analysis system. If needed, the same membrane was stripped with Restore Western blot stripping buffer and reblotted according to the protocol provided by Pierce (Rockford, IL).

Primary antibodies for western blotting were the following: anti-Pacsin 2 in[1] 1:15,000 dilution; anti-GAPDH (Santa Cruz Biotechnology, Santa Cruz, CA, FL-335 sc-25778) in 1:1000 dilution; anti-β-actin (Sigma-Aldrich, St Louis, MO, LLC. A2228) in 1:50,000 dilution; and anti-p44/42 MAPK (extracellular signal–regulated protein kinases 1 and 2) Antibody (Cell Signaling Technology, Danvers, MA, no. 9102) in 1:1000 dilution. Secondary antibodies (Amersham Pharmacia Biotech, Pittsburgh, PA) were used in a 1:5000 dilution.

Immunostaining and immunofluorescence microscopy

Cultured cells were fixed with 4% paraformaldehyde/3% sucrose and permeabilized with 0.3% Triton X-100. Permeabilized cells were blocked with either 5% bovine serum albumin or 10% goat serum for 1 h at room temperature, and then incubated with the primary antibodies for 1 h at room temperature or overnight at 4 °C. After washing with ice-cold phosphate-buffered saline, they were incubated with a labeled secondary antibody for 1 h at room temperature. Slides were mounted with ProLong Gold antifade reagent with 4',6-diamidino-2-phenylindole (Invitrogen, catalog no. P36935). A Nikon fluorescence microscope and the SPOT camera system were used for image analysis (Nikon, Tokyo, Japan).

Paraffin-embedded sections (4 mm), derived from perfused kidneys, were dewaxed, rehydrated through graded alcohols, and boiled for 30 min in 10 mmol/l citrate (pH 6.0; Vector Laboratories, Burlingame, CA). After cooling, the sections were blocked with 5%

bovine serum albumin or 10% goat serum for 1 h at room temperature and processed as cultured cells as mentioned above.

Primary antibodies for immunostaining were the following: Pacsin 2 in[1] 1:4000 dilution and antiacetylated-α-tubulin (Sigma- Aldrich, catalog no. T6793) in 1:40,000 dilution; fluorescent-labeled secondary antibodies were all from Invitrogen and used in a 1:500 dilution. Fluorescein DBA (Vector Laboratories, catalog no. FL-1031) in 1:500 dilution or fluorescein LTA (Vector Laboratories, catalog no., FL-1321) in 1:500 dilution was used to detect, respectively, collecting tubules/ducts or proximal tubules.

Renal IRI

The IRI surgery was performed as previously described.[21] Briefly, animals were anesthetized with pentobarbital sodium (60 mg/kg body weight, intraperitoneally) before surgery. Body temperatures were controlled at 36.5–37.5 °C throughout the procedure. Kidneys were exposed through flank incisions and mice were subjected to ischemia by clamping the left renal pedicle with nontraumatic microaneurysm clamps (Roboz, Rockville, MD), which were removed after 25 min (males) or 35 min (females). The right kidneys were severed as contralateral nonischemic (control) kidneys. At 2 h after surgery, 1 ml of 0.9% NaCl was administered subcutaneously.

Tubulogenesis analysis

mIMCD3 cells were cultured in collagen I 3D gels. The collagen mixture was prepared with 8 volumes of type I collagen stock solution (BD Bioscience, San Jose, CA), 1 volume of concentrated Dulbecco's modified Eagle's medium (Sigma-Aldrich), and 1 volume of 200 mmol/l HEPES (Sigma). mIMCD3 cells (4×10^3) were suspended in the collagen mixture (1 ml), and 0.85 ml of the mixture was transferred gently into six-well tissue culture plates. After incubating the cultures at 37 °C until the collagen solidified, 2 ml of growth medium with or without 40 ng/ml HGF was added (Sigma Chemical, St Louis, MO). The medium was changed every 2–3 days. Cells were observed by phase-contrast microscopy and photographed.

Invasion analysis

Invasion of mIMCD3 cells into type I collagen gels was analyzed as described previously.[11,30] Briefly, transwell filters (8-μm pore size, 6.5 mm diameter; Corning, Corning, NY) were coated with type I collagen by following the manufacturer's instruction. Cells (5×10^4) were seeded to the upper chambers without HGF, and the chambers were placed in 24-well tissue culture plates containing medium with HGF (20 ng/ml). After incubation at 37 °C for 16 h, cultures were washed with phosphate-buffered saline, fixed with ice-cold methanol, and stained with Giemsa staining solution. The bottom surface of the filter was photographed to detect the cells that had migrated through the filters.

MTT cell proliferation and FACS cell cycle analysis

To determine the cell proliferation rate of the Pacsin 2 knockdown and control mIMCD3 cells, 5000 cells were seeded in each well of a 24-well tissue culture plate. This was done in triplicate. The cells were stained with MTT at 0, 24, 48, and 72 h, and the absorption at 590

nm was determined with a microtiter plate reader (Molecular Devices, Sunnyvale, CA). For cell cycle profile analysis, cells were synchronized at G0 phase by serum starvation for 24 h, and then allowed to reenter the cell cycle by supplying 10% serum for an additional 24 h, and stained with propidium iodide. Cells were scored by the FACScan flow cytometer (Becton Dickinson, Franklin Lakes, NJ). Cell cycle distribution was analyzed with the Cellquest software (Becton Dickinson).

Supplementary Material

Refer to Web version on PubMed Central for supplementary material.

Acknowledgments

We thank the members of the Zhou Lab and of the Harvard Center for Polycystic Kidney Disease Research (P50DK074030) for scientific discussions and support. This work was supported by grants from the National Institutes of Health (DK40703, DK51050, and P50DK074030) to JZ. GY is a recipient of a postdoctoral fellowship from the American Heart Association, and AT is a recipient of a Scientist Development Grant from the American Heart Association.

REFERENCES

1. Modregger J, Ritter B, Witter B, et al. All three PACSIN isoforms bind to endocytic proteins and inhibit endocytosis. J Cell Sci. 2000; 113(Part 24):4511–4521. [PubMed: 11082044]
2. Wang Q, Navarro MV, Peng G, et al. Molecular mechanism of membrane constriction and tubulation mediated by the F-BAR protein Pacsin/Syndapin. Proc Natl Acad Sci USA. 2009; 106:12700–12705. [PubMed: 19549836]
3. Plomann M, Wittmann JG, Rudolph MG. A hinge in the distal end of the PACSIN 2 F-BAR domain may contribute to membrane-curvature sensing. J Mol Biol. 2010; 400:129–136. [PubMed: 20471395]
4. Frost A, Unger VM, De Camilli P. The BAR domain superfamily: membrane-molding macromolecules. Cell. 2009; 137:191–196. [PubMed: 19379681]
5. Edeling MA, Sanker S, Shima T, et al. Structural requirements for PACSIN/Syndapin operation during zebrafish embryonic notochord development. PLoS One. 2009; 4:e8150. [PubMed: 19997509]
6. Qualmann B, Kelly RB. Syndapin isoforms participate in receptor-mediated endocytosis and actin organization. J Cell Biol. 2000; 148:1047–1062. [PubMed: 10704453]
7. Merrifield CJ, Feldman ME, Wan L, et al. Imaging actin and dynamin recruitment during invagination of single clathrin-coated pits.[see comment]. Nat Cell Biol. 2002; 4:691–698. [PubMed: 12198492]
8. Kessels MM, Qualmann B. Syndapins integrate N-WASP in receptor-mediated endocytosis. EMBO J. 2002; 21:6083–6094. [PubMed: 12426380]
9. Baum B, Kunda P. Actin nucleation: spire - actin nucleator in a class of its own. Curr Biol. 2005; 15:R305–R308. [PubMed: 15854898]
10. Dharmalingam E, Haeckel A, Pinyol R, et al. F-BAR proteins of the syndapin family shape the plasma membrane and are crucial for neuromorphogenesis. J Neurosci. 2009; 29:13315–13327. [PubMed: 19846719]
11. Yamaguchi H, Miki H, Takenawa T. Neural Wiskott-Aldrich syndrome protein is involved in hepatocyte growth factor-induced migration, invasion, and tubulogenesis of epithelial cells. Cancer Res. 2002; 62:2503–2509. [PubMed: 11980641]
12. Merilainen J, Lehto VP, Wasenius VM. FAP52, a novel, SH3 domain-containing focal adhesion protein. J Biol Chem. 1997; 272:23278–23284. [PubMed: 9287337]
13. Plomann M, Lange R, Vopper G, et al. PACSIN, a brain protein that is upregulated upon differentiation into neuronal cells. Eur J Biochem. 1998; 256:201–211. [PubMed: 9746365]

14. Qualmann B, Roos J, DiGregorio PJ, et al. Syndapin I, a synaptic dynamin-binding protein that associates with the neural Wiskott-Aldrich syndrome protein. Mol Biol Cell. 1999; 10:501–513. [PubMed: 9950691]
15. Ritter B, Modregger J, Paulsson M, et al. PACSIN 2, a novel member of the PACSIN family of cytoplasmic adapter proteins. FEBS Lett. 1999; 454:356–362. [PubMed: 10431838]
16. Kessels MM, Qualmann B. The syndapin protein family: linking membrane trafficking with the cytoskeleton. J Cell Sci. 2004; 117:3077–3086. [PubMed: 15226389]
17. Badano JL, Mitsuma N, Beales PL, et al. The ciliopathies: an emerging class of human genetic disorders. Annu Rev Genomics Hum Genet. 2006; 7:125–148. [PubMed: 16722803]
18. Grimm-Gunter EM, Milbrandt M, Merkl B, et al. PACSIN proteins bind tubulin and promote microtubule assembly. Exp Cell Res. 2008; 314:1991–2003. [PubMed: 18456257]
19. Pollack AL, Runyan RB, Mostov KE. Morphogenetic mechanisms of epithelial tubulogenesis: MDCK cell polarity is transiently rearranged without loss of cell-cell contact during scatter factor/hepatocyte growth factor-induced tubulogenesis. Dev Biol. 1998; 204:64–79. [PubMed: 9851843]
20. Duffield JS, Bonventre JV. Kidney tubular epithelium is restored without replacement with bone marrow-derived cells during repair after ischemic injury. Kidney Int. 2005; 68:1956–1961. [PubMed: 16221175]
21. Takakura A, Contrino L, Zhou X, et al. Renal injury is a third hit promoting rapid development of adult polycystic kidney disease. Hum Mol Genet. 2009; 18:2523–2531. [PubMed: 19342421]
22. Grobstein C. Trans-filter induction of tubules in mouse metanephrogenic mesenchyme. Exp Cell Res. 1956; 10:424–440. [PubMed: 13317909]
23. Erickson RA. Inductive interactions in the development of the mouse metanephros. J Exp Zool. 1968; 169:33–42. [PubMed: 5696642]
24. Mori K, Yang J, Barasch J. Ureteric bud controls multiple steps in the conversion of mesenchyme to epithelia. Semin Cell Dev Biol. 2003; 14:209–216. [PubMed: 14627119]
25. Michael L, Sweeney DE, Davies JA. A role for microfilament-based contraction in branching morphogenesis of the ureteric bud. Kidney Int. 2005; 68:2010–2018. [PubMed: 16221201]
26. de Kreuk BJ, Nethe M, Fernandez-Borja M, et al. The F-BAR domain protein PACSIN2 associates with Rac1 and regulates cell spreading and migration. J Cell Sci. 2011; 124:2375–2388. [PubMed: 21693584]
27. Meng H, Tian L, Zhou J, et al. PACSIN 2 represses cellular migration through direct association with cyclin D1 but not its alternate splice form cyclin D1b. Cell Cycle. 2011; 10:73–81. [PubMed: 21200149]
28. Kim J, Lee JE, Heynen-Genel S, et al. Functional genomic screen for modulators of ciliogenesis and cilium length. Nature. 2010; 464:1048–1051. [PubMed: 20393563]
29. Guo P, Weinstein AM, Weinbaum S. A hydrodynamic mechanosensory hypothesis for brush border microvilli. Am J Physiol Renal Physiol. 2000; 279:F698–F712. [PubMed: 10997920]
30. Kong T, Xu D, Yu W, et al. G alpha 12 inhibits alpha2 beta1 integrin-mediated Madin-Darby canine kidney cell attachment and migration on collagen-I and blocks tubulogenesis. Mol Biol Cell. 2009; 20:4596–4610. [PubMed: 19776354]

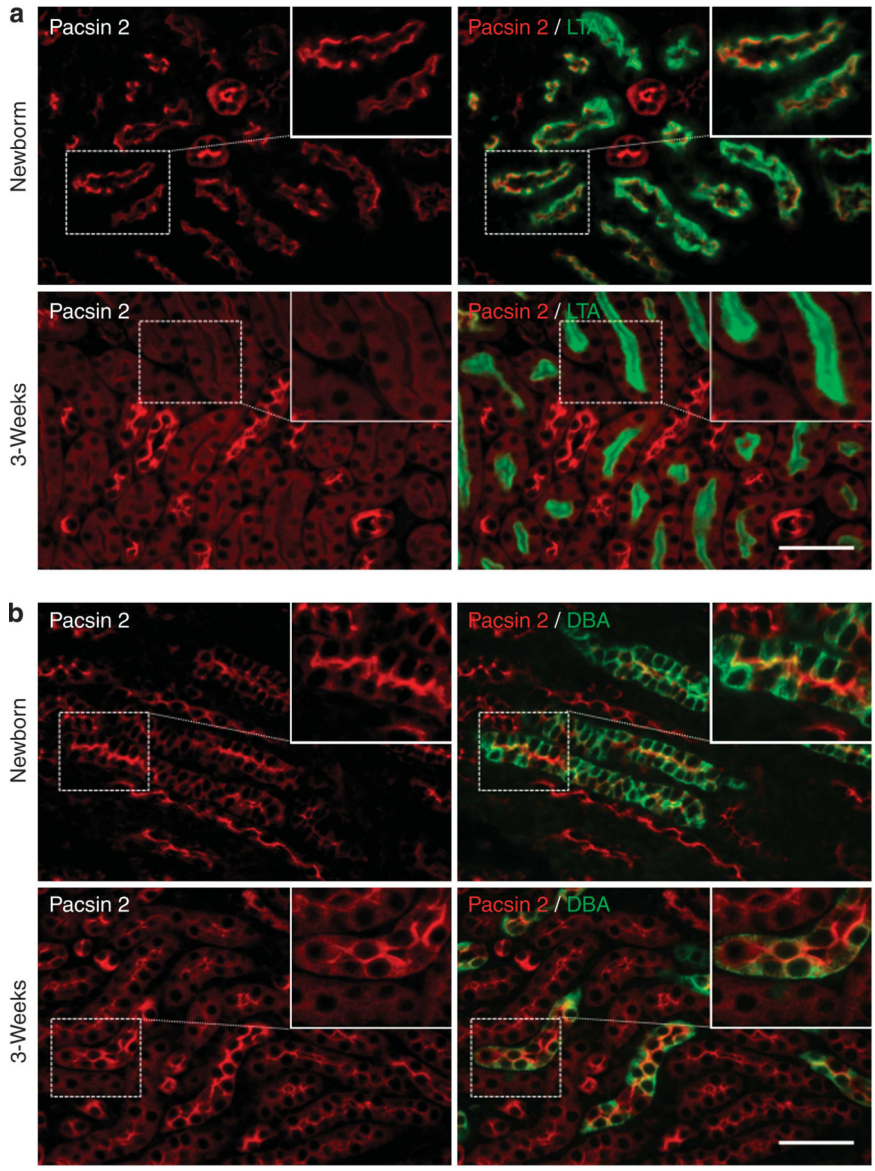

Figure 1. Pacsin 2 expression in Lotus tetragonolobus agglutinin–positive (LTA^+) proximal and Dolichos biflorus agglutinin–positive (DBA^+) collecting tubules in postnatal kidneys

(**a**) Strong Pacsin 2 expression in the apical membrane of LTA^+ proximal tubules in newborn mouse kidneys, which is remarkably reduced and becomes cytosolic in 3-week-old mouse kidneys. (**b**) Strong apical expression of Pacsin 2 in DBA^+ distal tubules in both newborn and 3-week-old kidneys. Insets show enlarged images of respective boxed areas. Bar=50 μm.

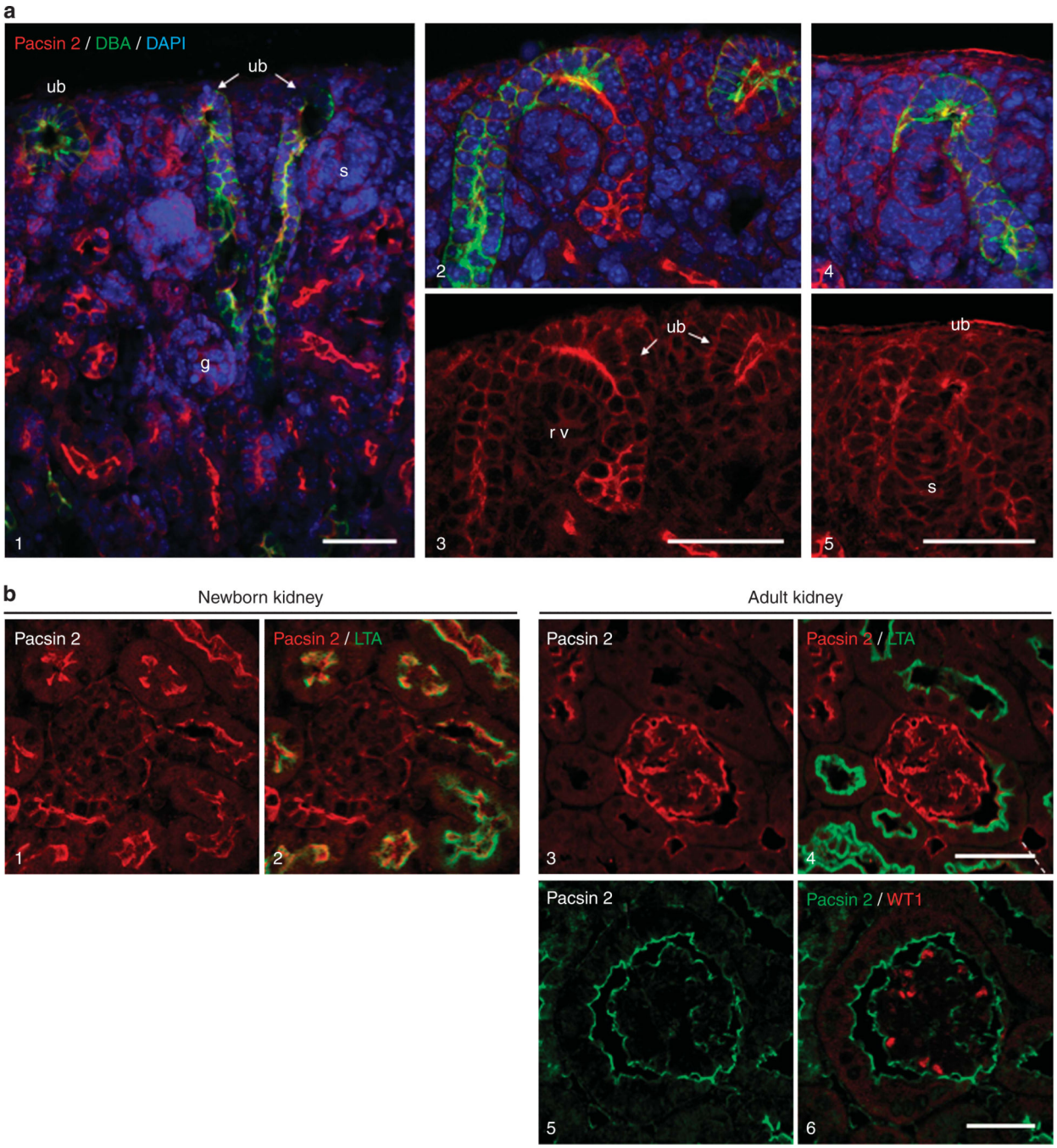

Figure 2. Pacsin 2 expression in the nephrogenic zone and in newborn and adult mouse kidney glomerulus

(**a**) Confocal images showing apical Pacsin 2 expression in the tips of ureteric bud–derived structures, but not in S-shaped bodies or renal vesicles. DAPI, 4',6-diamidino-2-phenylindole; g, glomerulus; rv, renal vesicle; s, S-shaped body; ub, ureteric bud. (**b**) In newborn mouse kidneys (1–2), Pacsin 2 is weakly expressed in the parietal epithelial cells of the Bowman's capsule and in the glomerular tufts. (3–6) There is a remarkable upregulation of Pacsin 2 in adult 3-month-old kidneys. (5–6) Confocal images showing the strong

expression of Pacsin 2 on the plasma membrane of podocytes of the glomerular tufts, which were labeled by WT1 staining. Bar = 50 μm.

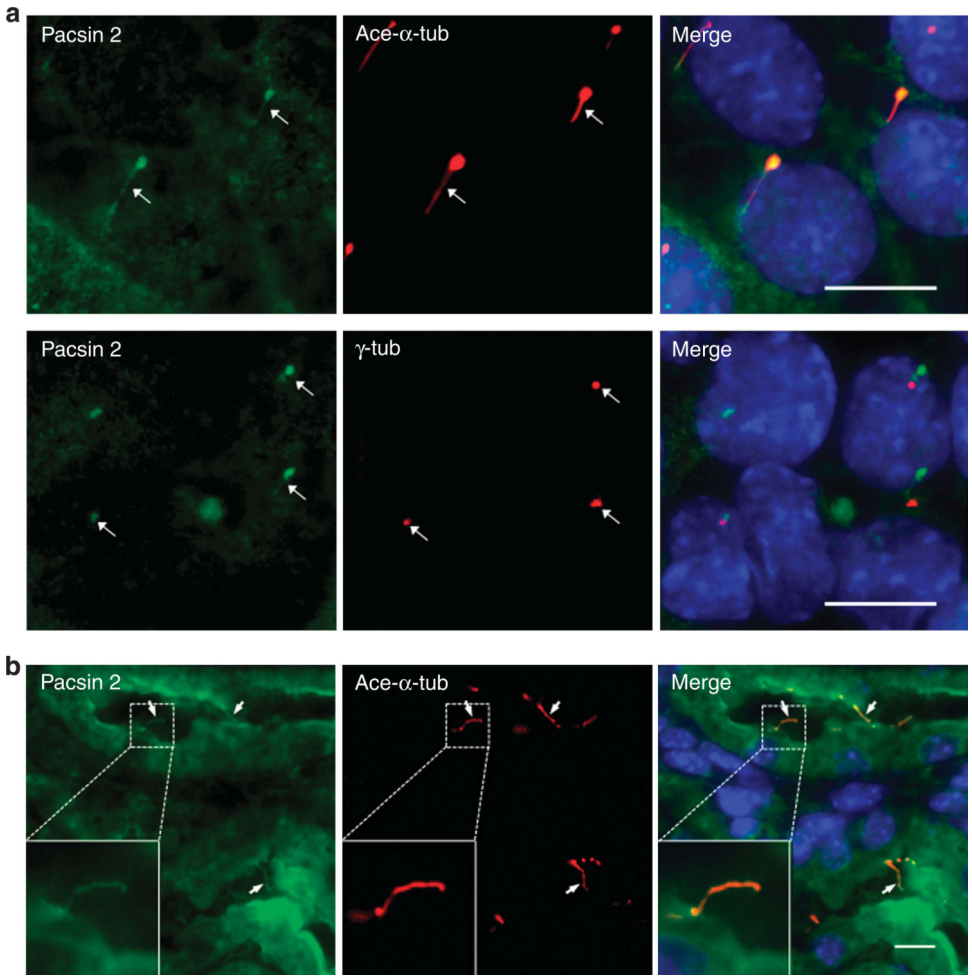

Figure 3. Pacsin 2 localizes on the primary cilia of kidney epithelial cells

(**a**) Pacsin 2 localizes on the primary cilia of murine inner medullary collecting duct 3 (mIMCD3) cells as indicated by a cilium axoneme marker acetylated-α-tubulin (top panels) and a basal body marker γ-tubulin (bottom panels). (**b**) Pacsin 2 is weakly expressed on the primary cilia of tubular epithelial cells in a neonatal kidney. Arrow points to the cilia. Bar = 10 μm.

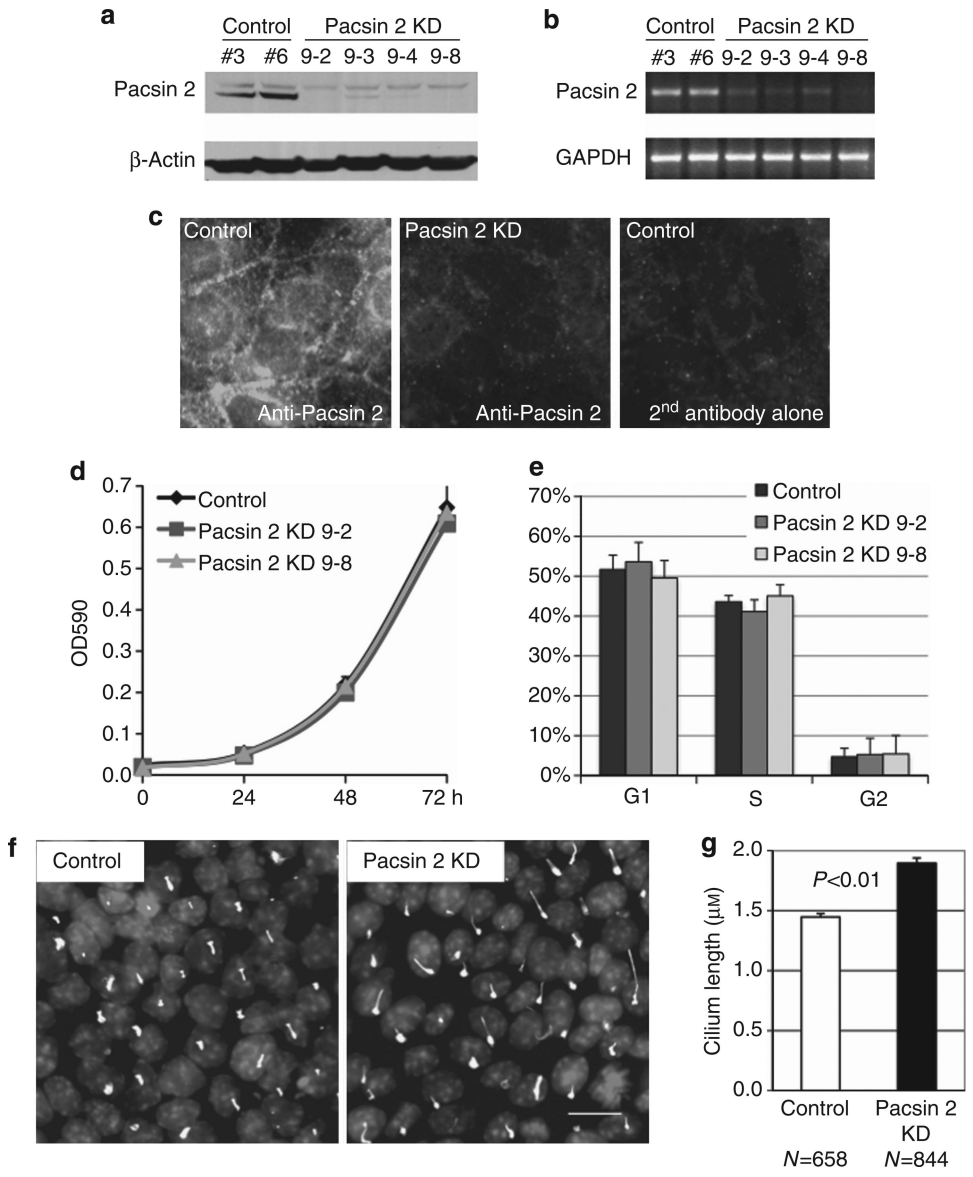

Figure 4. Establishment of stable lines of Pacsin 2 knockdown murine inner medullary collecting duct 3 (mIMCD3) cells by small hairpin RNA (shRNA)

(**a**) Western blot and (**b**) semiquantitative PCR demonstrate a significant reduction in the Pacsin 2 expression levels in four stable Pacsin 2 knockdown mIMCD3 clones, compared with the pSilencer control clones. GAPDH, glyceraldehyde-3-phosphate dehydrogenase. (**c**) Immunofluorescent images show that the apical localization of Pacsin 2 is significantly reduced in Pacsin 2 knockdown mIMCD3 cells. Secondary antibodies alone were used as a control for the specificity of the Pacsin 2 antibody. (**d**) MTT (3-[4,5-dimethylthiazol-2-yl]-2,5-diphenyl-tetrazolium bromide) assay and (**e**) fluorescence-activated cell sorting (FACS) analyses show that the cell proliferation rate and the cell cycle profile are similar between stable Pacsin 2 knockdown and control mIMCD3 cell lines. (**f**) Pacsin 2 knockdown mIMCD3 cells process longer primary cilia as compared with control cells. The primary cilia axoneme was stained by acetylated α-tubulin. Bar = 10 μm. (**g**) Graph

demonstrating the length of the primary cilium. Control cells had an average cilium length of 1.45 μm (n = 658) as compared with 1.90 μm (n = 844) in knockdown cells. Error bars represent ± s.d. (n = 3). The significance was calculated by Student's t-test.

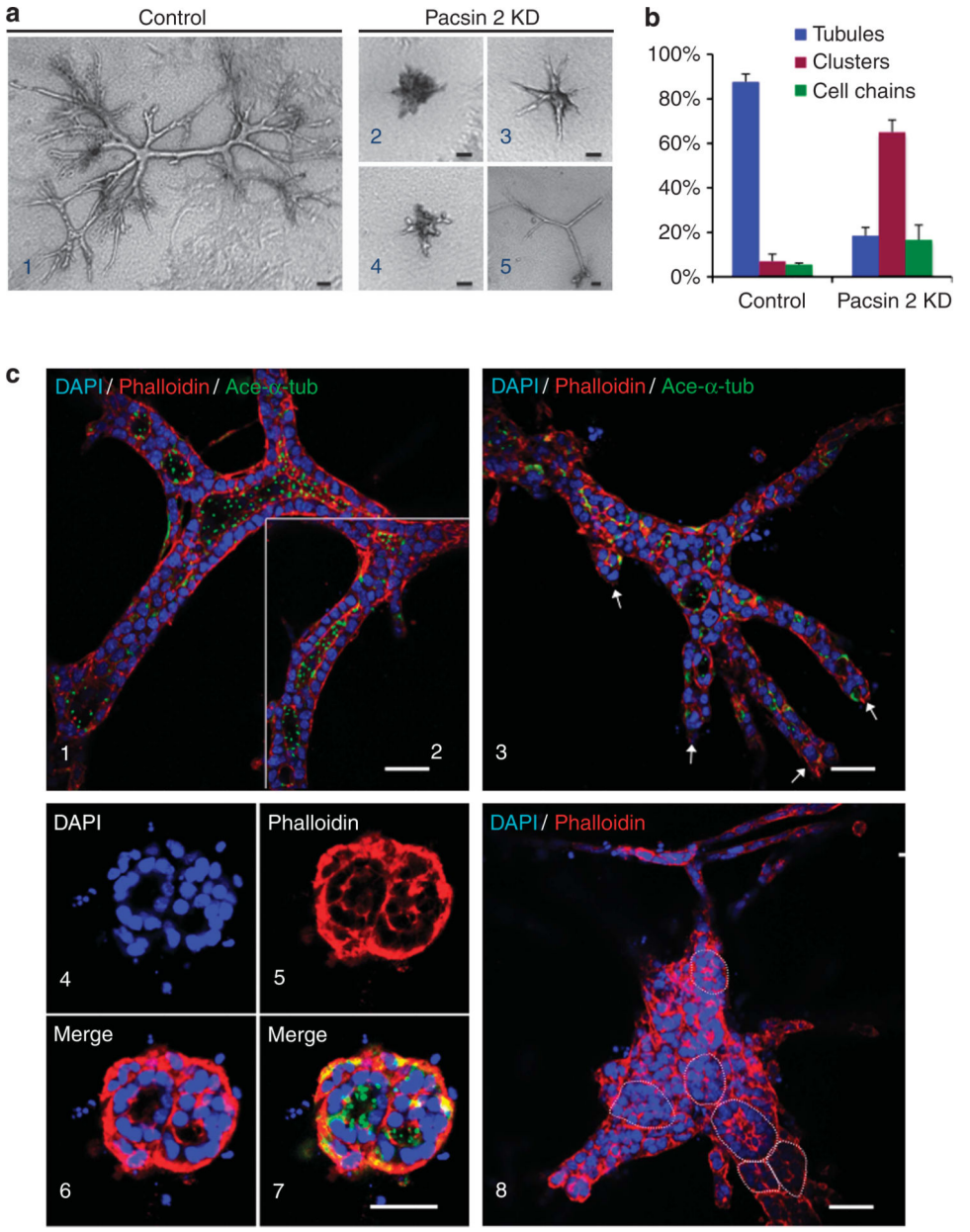

Figure 5. Pacsin 2 depletion leads to defects in tubulogenesis in three-dimensional (3D) collagen gels

(**a**) Phase-contrast images for (1) control and (2–5) Pacsin 2 knockdown murine inner medullary collecting duct 3 (mIMCD3) cells cultured for 12 days in 3D type I collagen gels. (**b**) Quantification of structures formed in 3D tubulogenesis assays. The structures formed in 3D collagen gels were classified into three categories (tubule, cell cluster, and cell chain). The percentage of each type of the structures was calculated by dividing by total number of structures formed. Cell structures were counted from four individual experiments. More than 160 structures were counted for each cell type. Error bars represent±s.d. (**c**) Confocal images of cells cultured in **a** stained with phalloidin and acetylated α-tubulin (ace-α-tub; green). DAPI, 4’,6-diamidino-2-phenylindole. (1–2) Control mIMCD3 cells formed large

elaborately branched tubular structures with well-established lumen lined with a single layer of epithelial cells with apical primary cilia protruding toward the lumen. The lumen for the tubule in (1) and (2) are connected, shown by two confocal optical sections that are 2 μm apart in the focal plane. (3–8) Pacsin 2 knockdown cells have defects in tubule formation. They tend to form tubules with blunt ends (3, arrows point to the blunt ends), or cell clusters with isolated lumens or multi-lumens (4–8). (4–7) Typical multilumen structures seen in Pacsin 2 knockdown mIMCD3 cells. (8) A large structure with at least six isolated lumens. Circle outlines the lumen. Bar = 50 μm.

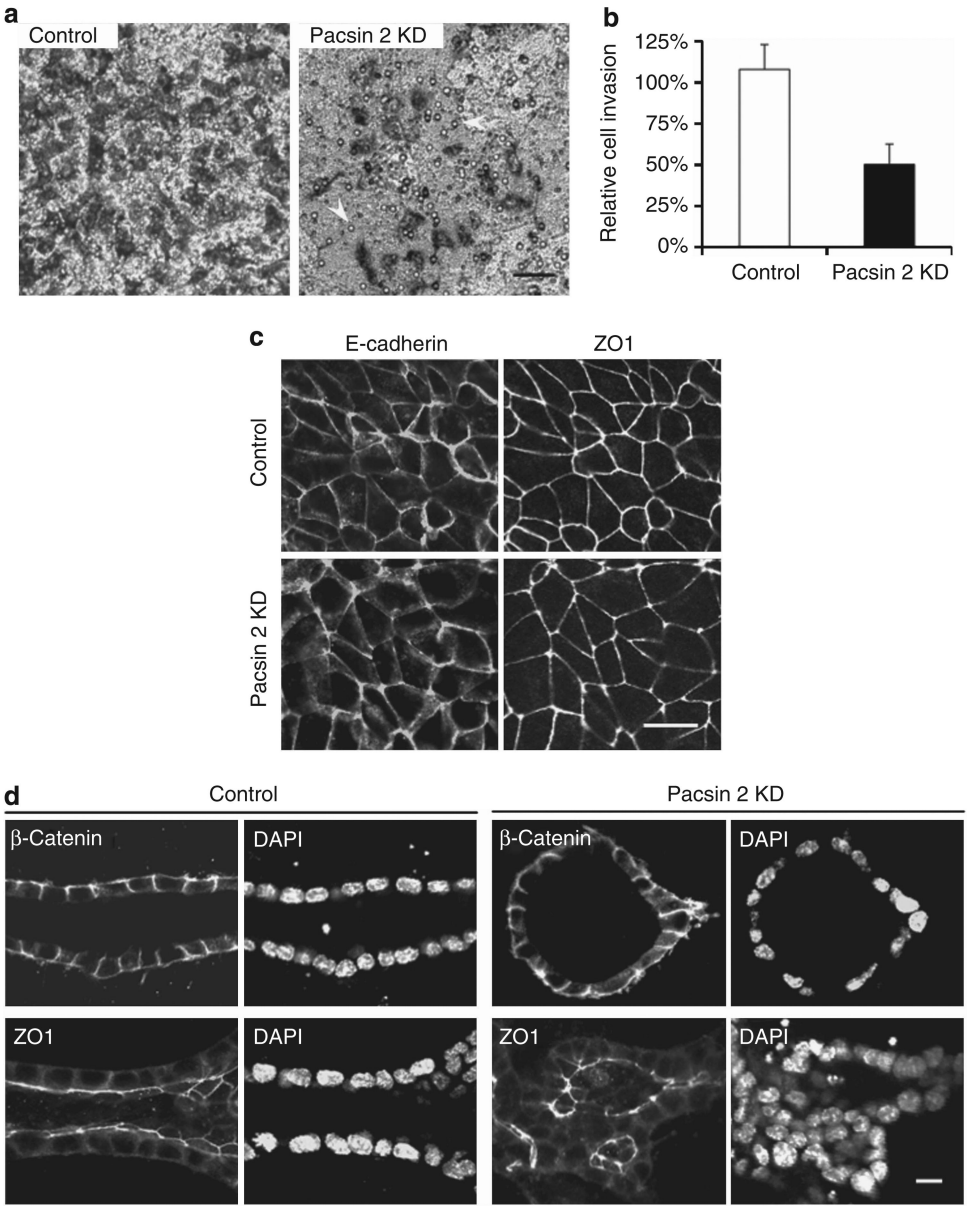

Figure 6. Pacsin 2 knockdown causes defects in cell invasion but not apical–basal polarity

(**a**) Equal number of Pacsin 2 knockdown cells and control murine inner medullary collecting duct 3 (mIMCD3) cells were seeded into the apical chamber of collagen I–coated transwell filters (8 μm) and allowed to travel to the underside of the filters for 16 h. Hepatic growth factor (HGF; 20 ng/ml) was added to the lower chamber. Migrated cells were stained by Giemsa and photographed with an inverted phase-contrast microscope. Arrows mark pores within the surface of the filter. Bar = 50 μm. (**b**) Quantification of cell invasion. The number of cells traveled to the basal surface in 12 separated fields were counted and divided by the starting number of cells. The control mIMCD3 cells were used for reference and set at 100%. Depleting Pacsin 2 impaired mIMCD3 cell travel through a permeable membrane. Error bars represent±s.d. (n = 3). The significance was calculated by Student's t-test. $P<0.01$. (**c**) Pacsin 2 knockdown and control mIMCD3 cells exhibit normal tight junctions and cell–

cell adhesions as analyzed by confocal microscopy. Tight junctions are labeled with ZO1, whereas cell–cell adhesions are stained with E-cadherin. Bar = 10 μm. (**d**) In 3D collagen gels, both ZO1 and β-catenin preserved a normal localization in structures formed by Pacsin 2 knockdown mIMCD3 cells as compared with tubules formed by control mIMCD3 cells in a tubulogenesis assay. DAPI, 4',6-diamidino-2-phenylindole. Bar 10 = μm. A color version of **c, d** with Z-stack images for **c** is shown in Supplementary Figure S4 online.

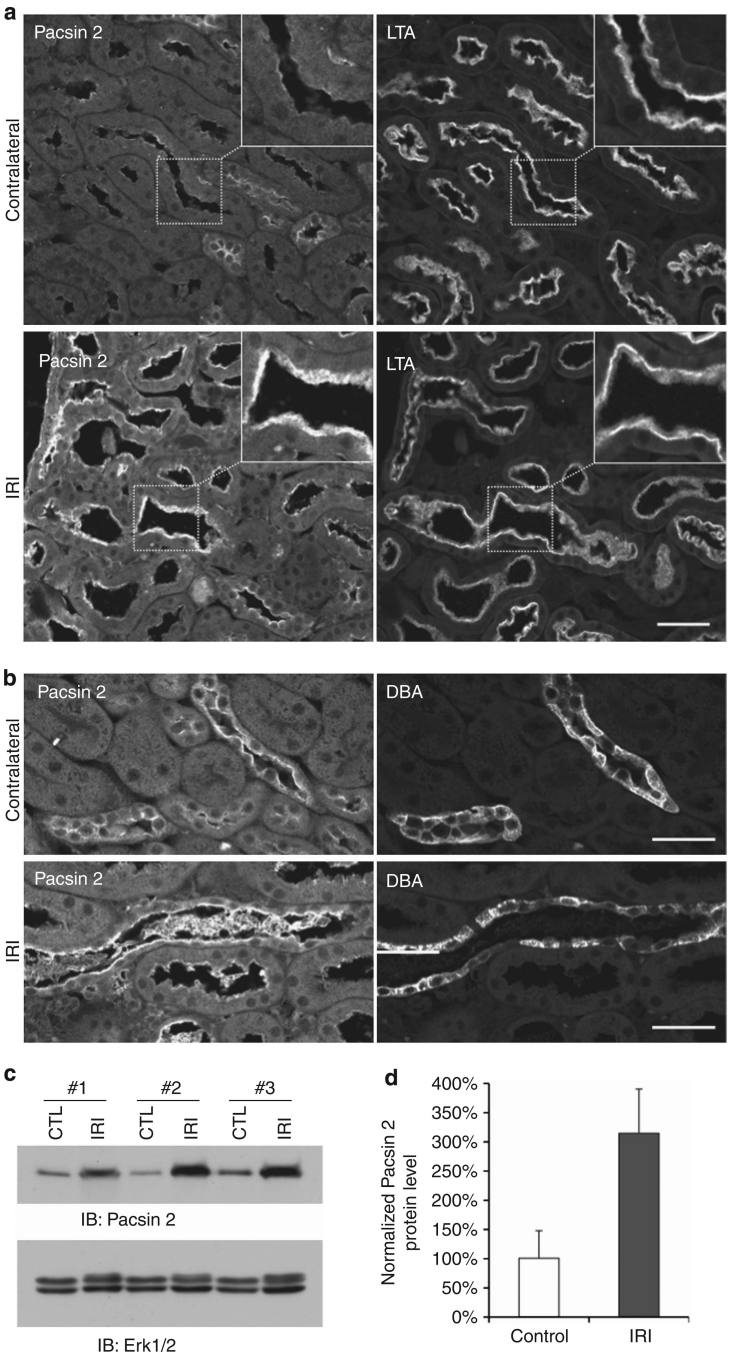

Figure 7. Pacsin 2 expression in normal and ischemia–reperfusion injured (IRI) kidneys

(**a**) Pacsin 2 expression is significantly upregulated in Lotus tetragonolobus agglutinin–positive (LTA^+) proximal tubules ischemic kidney compared with nonischemic kidneys, especially in the brush border (insert). Insets show enlarged images of the respective boxed areas. (**b**) Apical Pacsin 2 expression is also increased in Dolichos biflorus agglutinin–positive (DBA^+) collecting tubules in ischemic kidneys. Bar = 50 μm. (**c**) Pacsin 2 protein levels were remarkably increased in IRI kidneys compared with the nonischemic control (CTL) kidneys. Total Erk1/2 (extracellular signal–regulated protein kinases 1 and 2) was

used as loading control in this experiment. Three pairs of kidneys were used. For each kidney, half was used for immunofluorescence analysis in Figure 7a and b and the other half for western blotting. (**d**) The protein levels of Pacsin 2 were normalized to those of total Erk1/2 in each kidney, and the nonischemic control kidneys were used as reference and set at 100%. Error bars represent±s.d. (n = 3). The significance was calculated by Student's t-test. $P<0.05$.